Supporting information

Intercalation of Bismuth Nanoparticles into Ti_3C_2 MXene as Anode Materials for Lithium-Ion Batteries

Mengxiang Chen, ‡[a] Kai Li, ‡[a] Yanqinpeng Lu,[a] Guoyin Zhu,* [a, b] and Yizhou Zhang* [a,]

[a] Institute of Advanced Materials and Flexible Electronics (IAMFE) School of Chemistry and Materials Science, Jiangsu Key Laboratory of New Energy Devices & Interface Science, Reading Academy, Nanjing University of Information Science & Technology Nanjing, 210044, China. E-mail: yizhou.zhang@nuist.edu.cn; gyzhu@nuist.edu.cn

[b] State Key Laboratory of Coordination Chemistry, Nanjing University, Nanjing, Jiangsu, 210023 P.R. China

Table of Contents

1. General information

Characterizations

The morphology of the material was characterized using scanning electron microscopy (SEM, ZEISS, Gemini300S), and the elemental distribution was analyzed via energy-dispersive spectroscopy (EDS). The microstructure and crystallinity of the sample were determined using transmission electron microscopy (TEM, EM-2100F microscope) and high-resolution TEM (HRTEM). The crystal structure of the sample was determined using an X-ray diffractometer (XRD, Rigaku Ultra 250) with Cu Kα radiation (λ=1.5406 Å), in a 2θ range of 5° to 80°, at a scan speed of 10° min^{-1}. The surface elemental valence states and chemical compositions of the product were analyzed using an X-ray photoelectron spectrometer (XPS, Thermo Kalpha) with Al Kα radiation as the excitation source. N_2 adsorption-desorption isotherms of the sample were studied using a gas adsorption analyzer (Micromeritics Tristar II 3020) at a pretreatment temperature of 100 °C. The specific surface area (SSA) and pore size distribution were calculated using the Brunauer-Emmett-Teller (BET, Micromeritics ASAP2460) method and the Barrett-Joyner-Halenda (BJH) model, respectively.

Electrochemical measurements

All electrochemical performances were examined at room temperature. To evaluate the electrochemical performance of the Bi/MXene nanosheets, the working electrodes were fabricated by mixing 70 wt.% active material (the as-prepared Bi/MXene nanosheets), 20 wt.% conductive additive (superconductive carbon black, SCCB, Canrd), and 10 wt.% binder (polyvinylidene fluoride, PVDF, Canrd). The mixture was homogenously ground using a mortar and pestle for 30 minutes and

subsequently dispersed in N-methyl-2-pyrrolidinone (NMP, Aladdin). After continuously stirrying for 72 hours, the slurry was coated onto the current collecters (copper foils), followed by drying at 60 ℃ for 12 h in vacuum. The mass loading of the active material was 0.3–0.6 mg per slice (effective electrode area is 1.50 cm^2). After that, CR2032-type half cells were assembled in an argon-filled glovebox (MIKROUNA, the levels of H_2O and O_2 are below 0.1 ppm), using the resultant working electrodes, lithium foils as the counter and reference electrodes, microporous polypropylene films as a separator. 1.0 M $LiPF_6$ in a mixture of ethylene carbonate (EC), dimethyl carbonate (DMC), and ethyl methyl carbonate (EMC) (the volume ratio of EC/DMC/EMC was 1.0: 1.0: 1.0, battery grade) as the electrolyte. In the procedures of cell fabrication, 70 uL of electrolyte was used in each cell.

Taking advantage of CHI 660d, the CV measurements were performed between 0.01 and 3.00 V (vs Li/Li^+), and the EIS results were obtained at an AC voltage of 5 mV amplitude in the range of 100 kHz to 1 Hz. Galvanostatic charge-discharge stability and rate capability were carried out by Neware (CT/CTE-4000) at different current densities in the voltage range of 0.01-3.00 V (vs Li/ Li^+).

The charge storage kinetics of *L* were investigated based on the following relationship:[1]

$$i = av^b \qquad \text{* MERGEFORMAT (1)}$$

where *a* and *b* are constants. A b-value of 1 indicates a surface-controlled capacitive behavior dominated by Faradaic reactions, while a b-value of 0.5 corresponds to a diffusion-controlled process involving lithium-ion intercalation and transport. By taking the logarithm of both sides, the equation can be rearranged as:

$$\log(i) = b\log(v) + \log(a) \quad \text{* MERGEFORMAT (2)}$$

$$y = bx + c \quad \text{* MERGEFORMAT (3)}$$

To investigate the electrochemical reaction kinetics of the Bi/MXene electrode, GITT measurements were performed. During testing, both Bi/MXene and MXene electrodes were subjected to current pulses of 100 mA g^{-1} for 10 mins, followed by a 30-minute relaxation period to reach a quasi-equilibrium state. The lithium-ion diffusion coefficient (D_{Li}) within the electrodes was calculated using the following equation:[2, 3]

$$D_{Li} = \frac{4}{\pi\tau}\left(\frac{n_m V_M}{S}\right)^2\left(\frac{\Delta E_S}{\Delta E_\tau}\right)^2 \quad \text{* MERGEFORMAT (4)}$$

The term n_m represents the number of moles of active material, τ is the relaxation time, V_M denotes the molar volume of the electrode material, and S is the surface area of the electrode. ΔE_s refers to the total voltage change after a current pulse and subsequent relaxation, while ΔE_τ indicates the voltage change during the current pulse.

2. Material synthesis

Preparation Ti_3C_2 MXene Nanosheets

Typically, LiF (1.0 g) and HCl (21 mL, 9 M) were mixed in a plastic bottle. After stirring, the mixture was preheated in an oil bath at 50 °C for 5 minutes. Subsequently, Ti_3AlC_2 MAX (1.0 g) was gradually added to the plastic bottle under continuous stirring. The plastic bottle containing the sample was then returned to the oil bath at 50 °C for 45 hours. After the heating process, the resulting dispersion was washed via centrifugation at 3500 rpm until turbidity was achieved. Finally, the dispersion was treated with 20 mL of an aqueous LiCl solution (1.0 g) under ultrasonication for 1 hour, followed by centrifugation for 30 minutes to isolate MXene nanosheets. The sample was frozen overnight in a refrigerator and subsequently freeze-dried to yield the final MXene nanosheets.

Preparation of Bi/Ti_3C_2 MXene

MXene and $Bi(NO_3)_3$ were dispersed in 20 mL of deionized water and stirred for 12 h, followed by ultrasonication for 30 min. Afterward, 60 mg of $NaBH_4$ was added, and the mixture was stirred continuously for another 48 h. The resulting product was washed thoroughly with deionized water and ethanol, then dried at 60 °C to yield the Bi/MXene composite.

To investigate the influence of Bi content, a series of Bi/MXene composites were prepared by varying the amount of $Bi(NO_3)_3$ while keeping the MXene content constant at 200 mg. Specifically, 120, 180, and 240 mg of $Bi(NO_3)_3$ were used to prepare samples denoted as Bi/MXene-L, Bi/MXene, and Bi/MXene-H, respectively. All syntheses were conducted in 20 mL of deionized water under identical conditions.

3. Experimental data

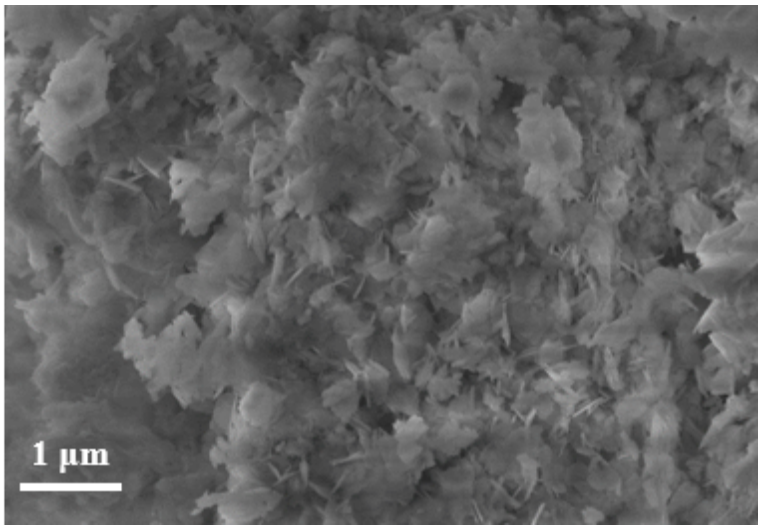

Fig. S1 SEM image of bare Bi.

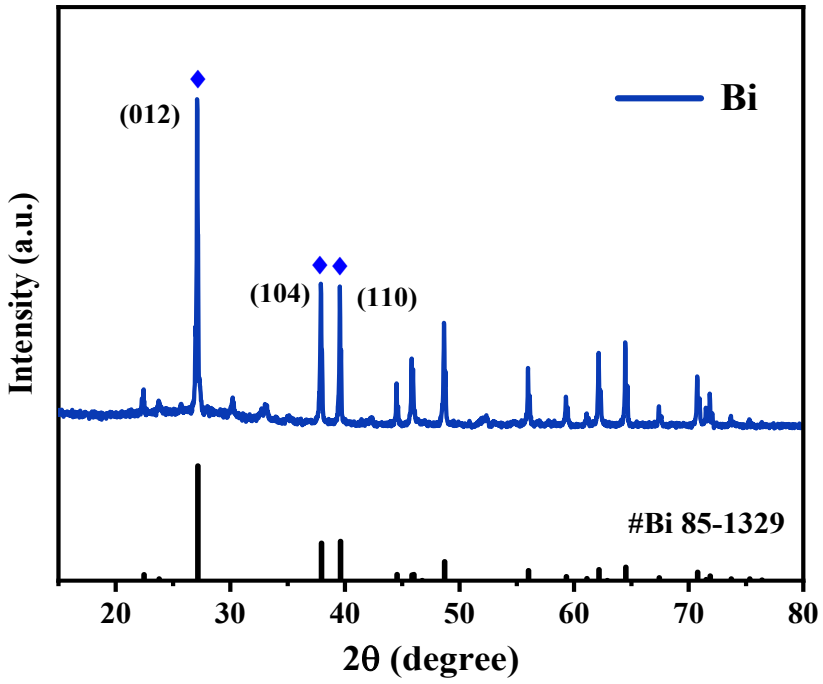

Fig. S2 XRD spectrum of bare Bi.

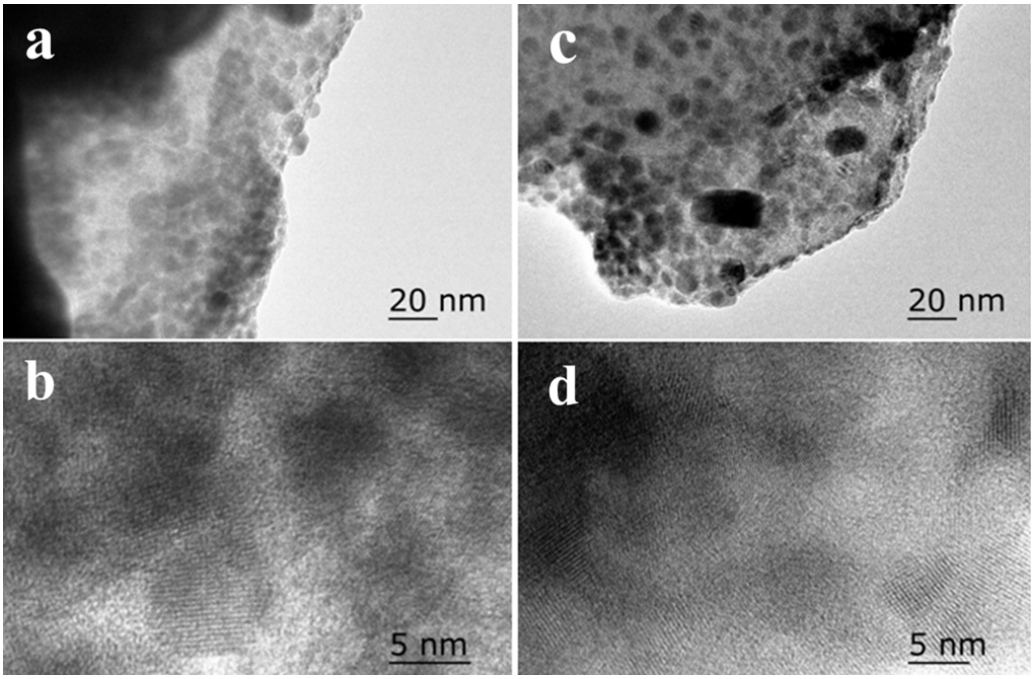

Fig. S3 TEM and HRTEM images of Bi/MXene composites synthesized with different $NaBH_4$ concentrations: (a, b) 60 mg $NaBH_4$ and (c, d) 120 mg $NaBH_4$.

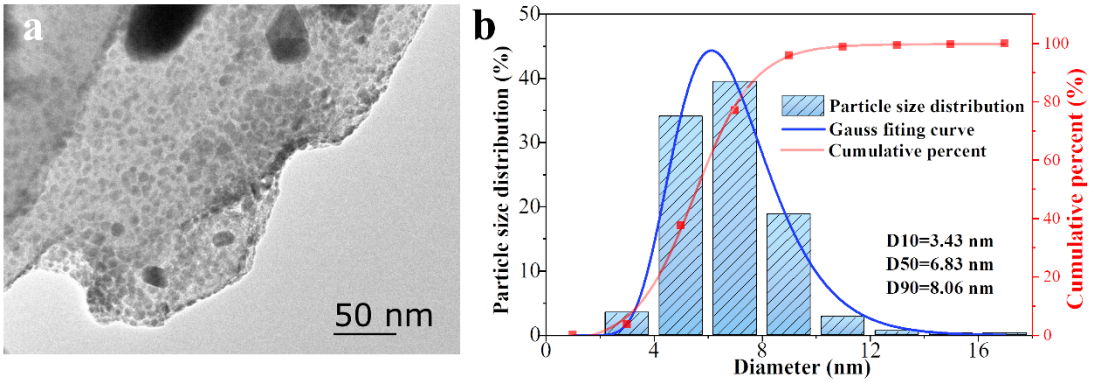

Fig. S4 (a) TEM image of the Bi/MXene composite. (b) Particle size distribution of Bi nanoparticles in the Bi/MXene composite based on statistical analysis from multiple TEM regions.

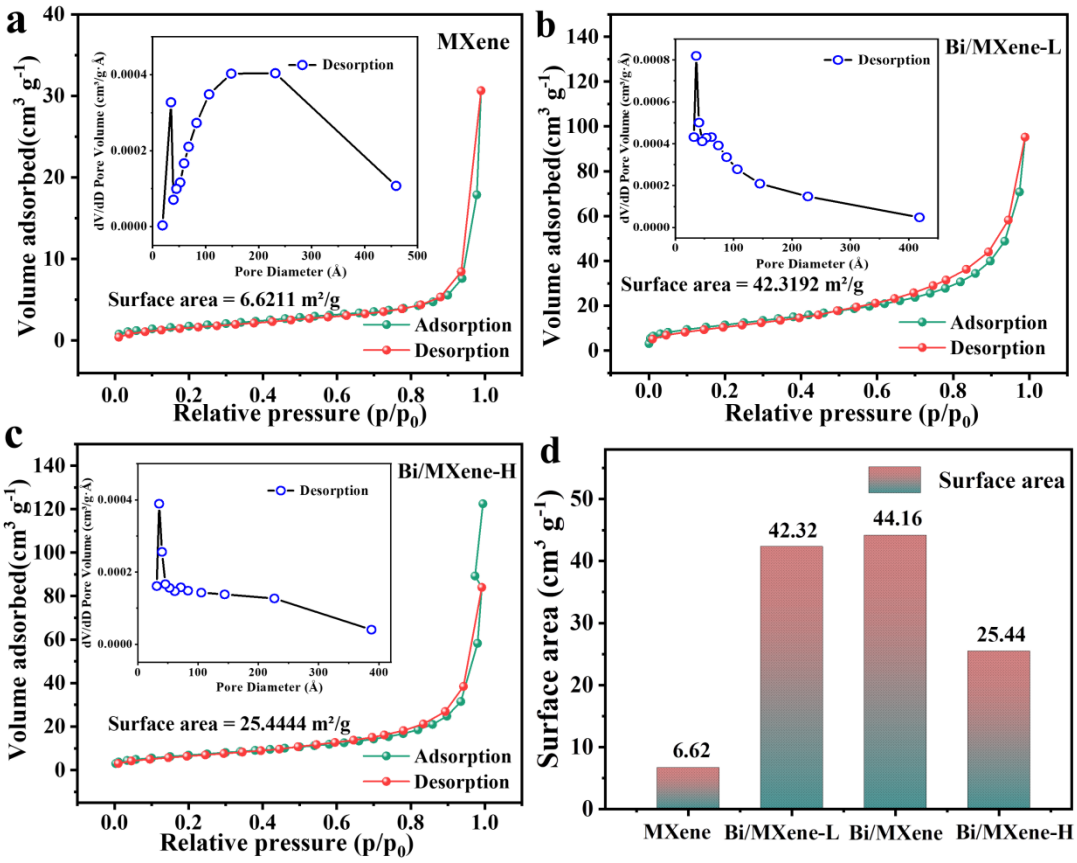

Fig. S5 N_2 adsorption-desorption isotherms and pore size distributions of (a) MXene, (b) Bi/MXene-L, (c) Bi/MXene-H, (d) comparison of specific surface areas of MXene and various Bi/MXene composites.

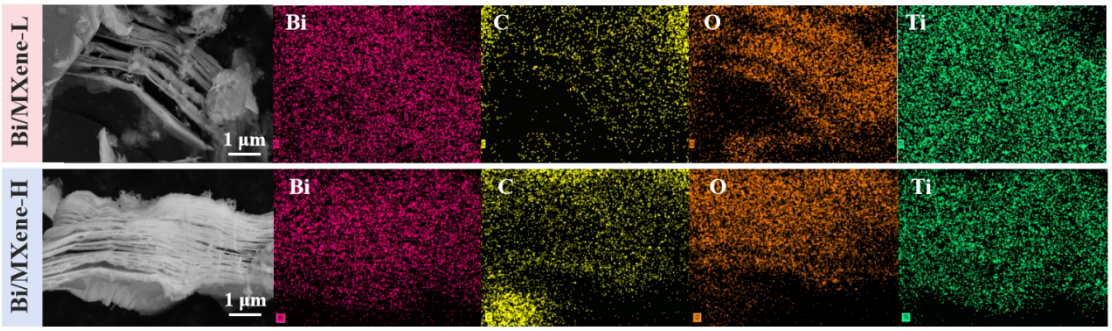

Fig. S6 SEM images and elemental mappings of Bi/MXene composites with different Bi contents.

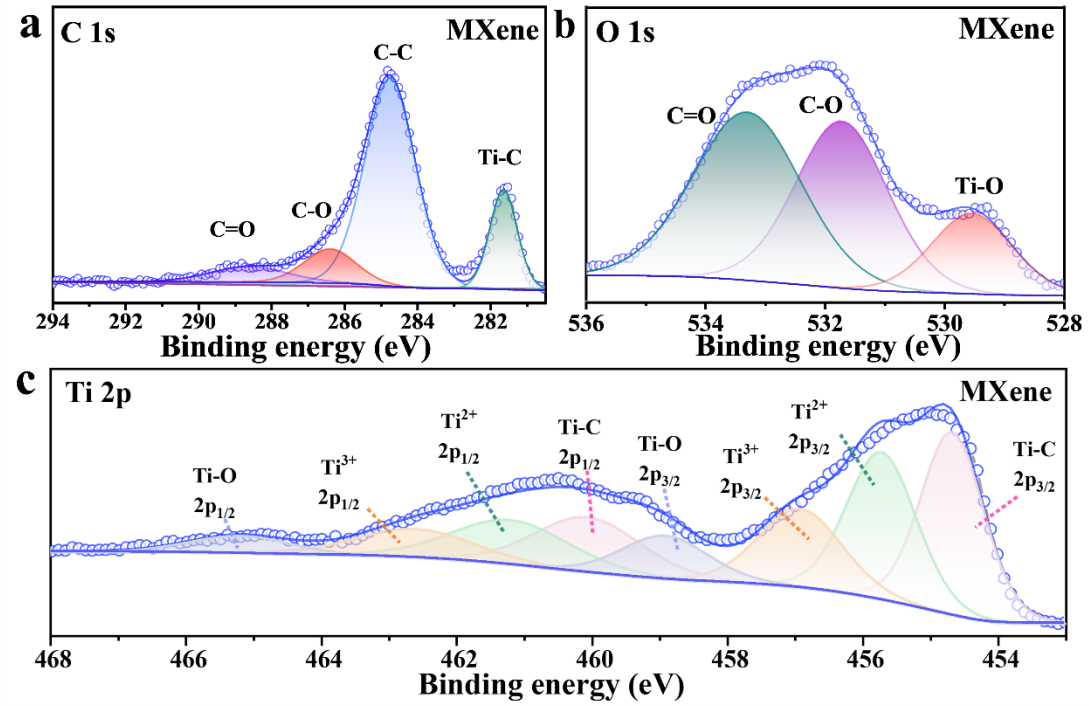

Fig. S7 XPS spectra of MXene: (a) C 1s, (b) O 1s, and (c) Ti 2p regions.

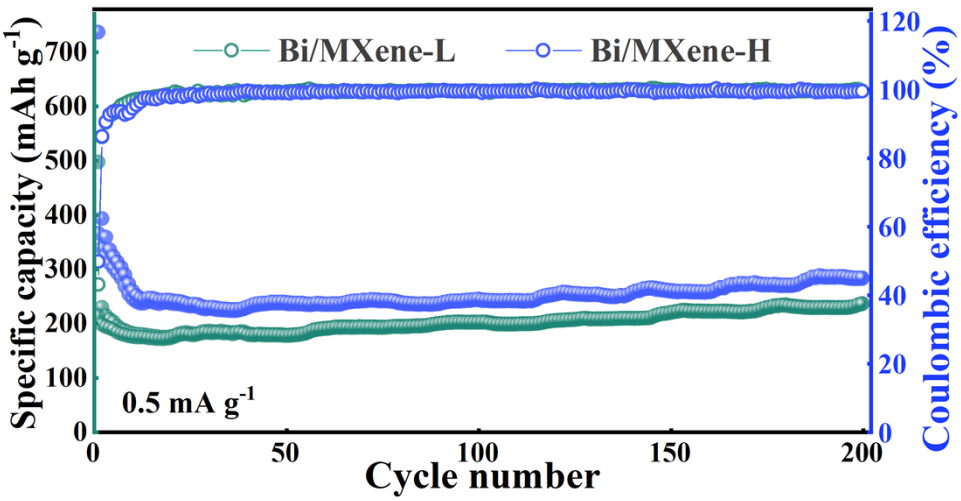

Fig. S8 Long-term cycling performance of Bi/MXene-L and Bi/MXene-H composites.

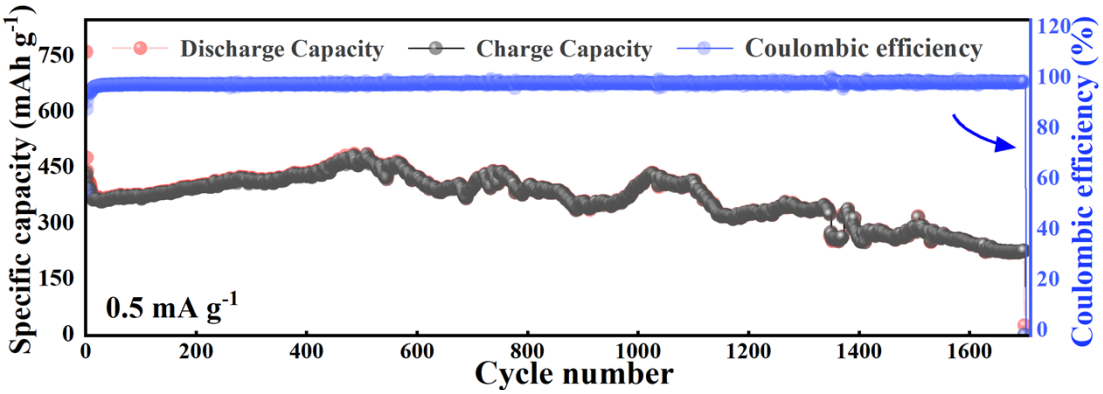

Fig. S9 Long-term cycling stability of Bi/MXene at 0.5 A g^{-1}.

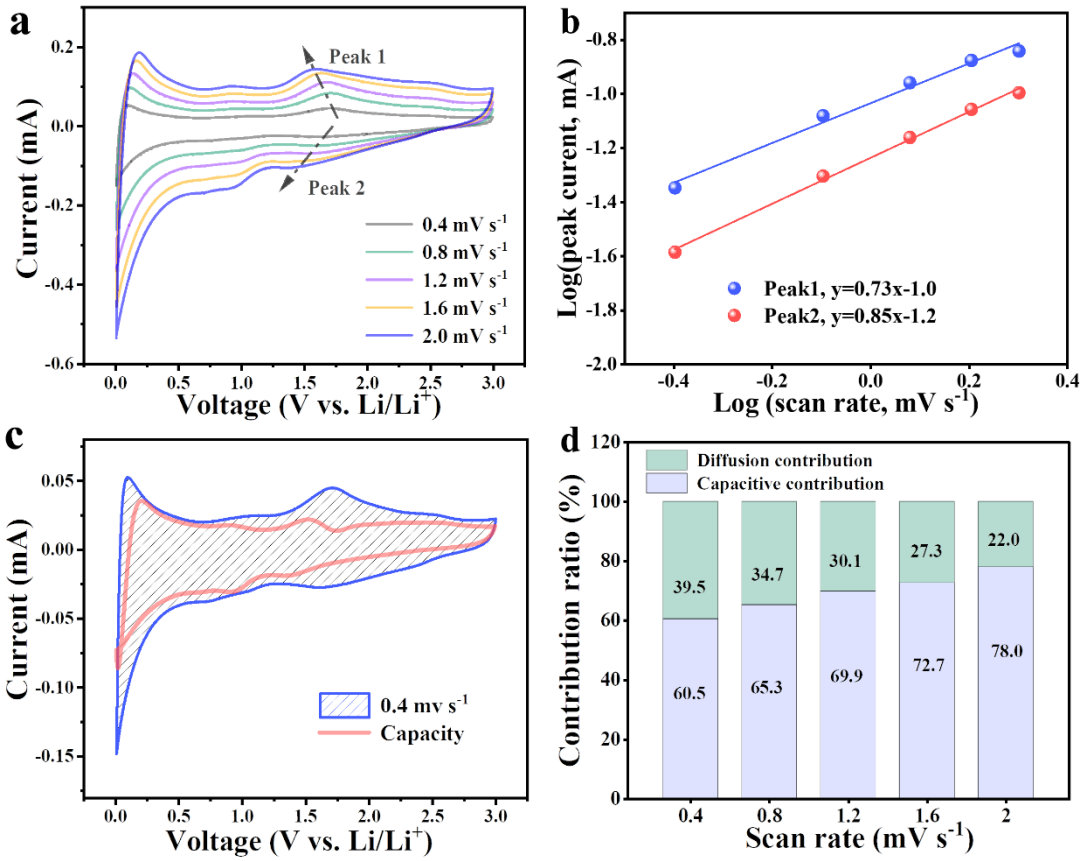

Fig. S10 Electrochemical kinetics analysis of MXene: (a) Sweep rate CV curves, (b) Line relationship of log(i) vs. log(v) plots, (c) capacitive contribution at 0.4 mV s^{-1}, (d) different scan rates capacitive contributions.

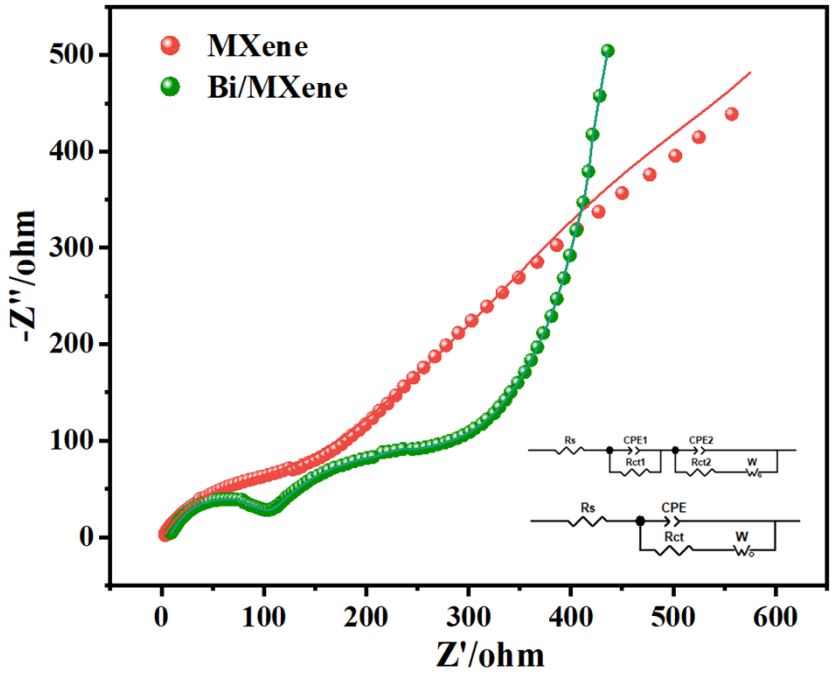

Fig. S11 The Nyquist plots of impedance spectra of Bi/MXene and MXene electrode before cycling.

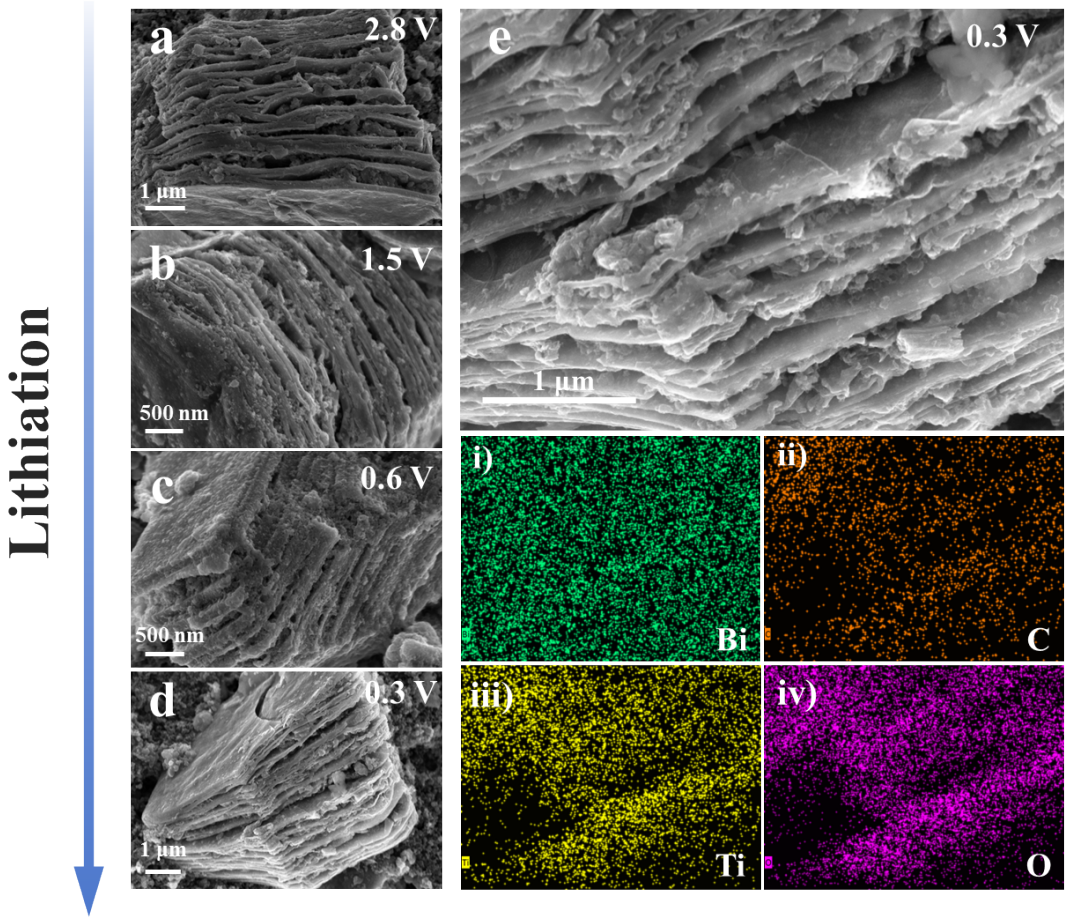

Fig. S12 SEM images of the Bi/MXene electrode collected at different discharge cut-off voltages: (a) 2.8 V, (b) 1.5 V, (c) 0.6 V, (d) 0.3 V, and (e) magnified SEM and corresponding EDS mapping at 0.3 V.

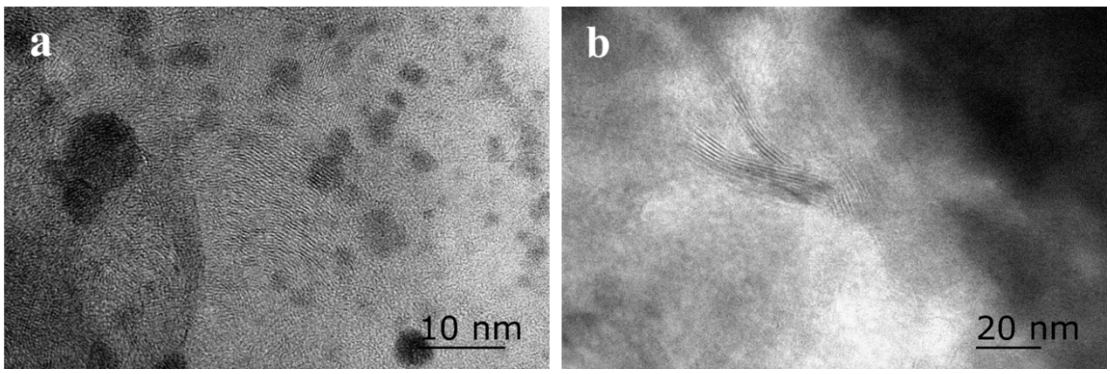

Fig. S13 TEM images of (a) Bi/MXene composite and (b) pristine MXene after 1000 charge–discharge cycles.

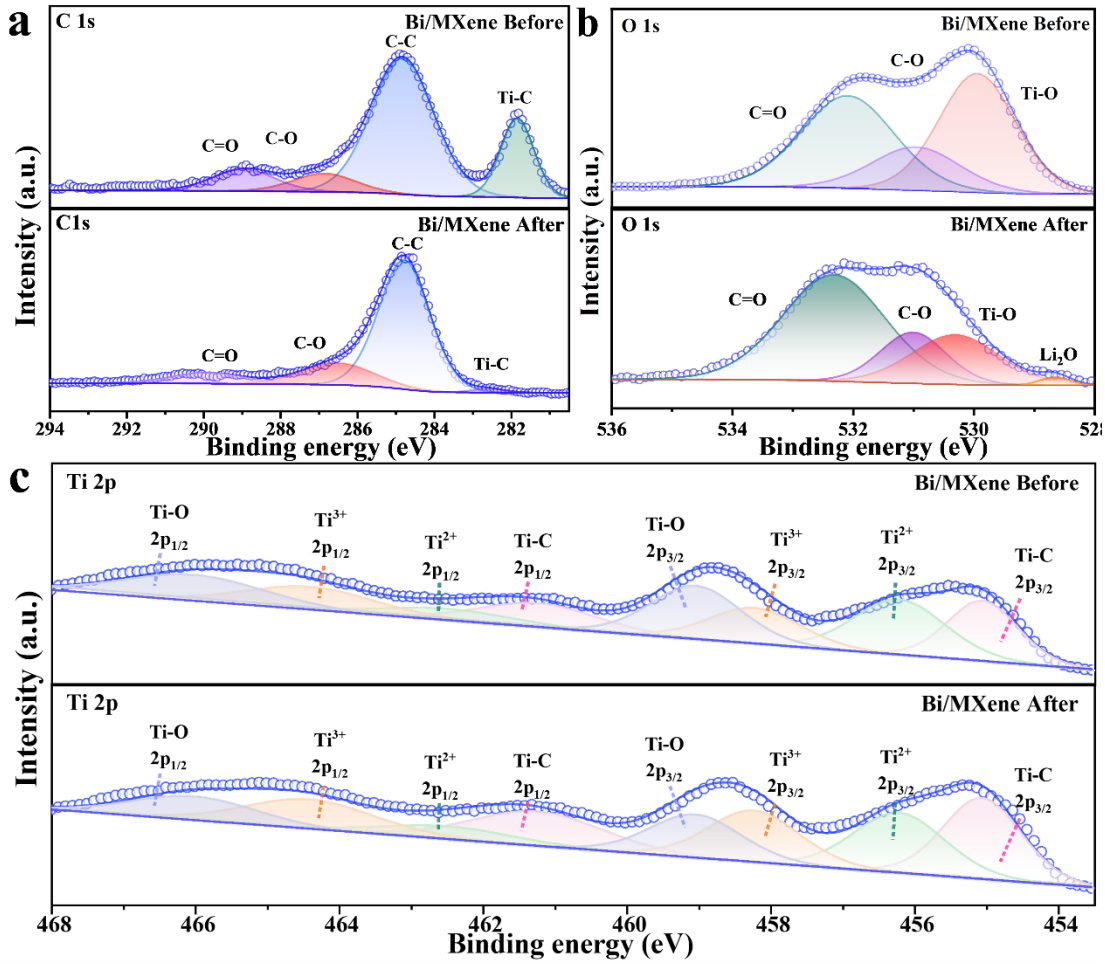

Fig. S14 XPS spectra of Bi/MXene before and after 1000 charge–discharge cycles. (a) C 1s, (b) O 1s and (c) Ti 2p regions.

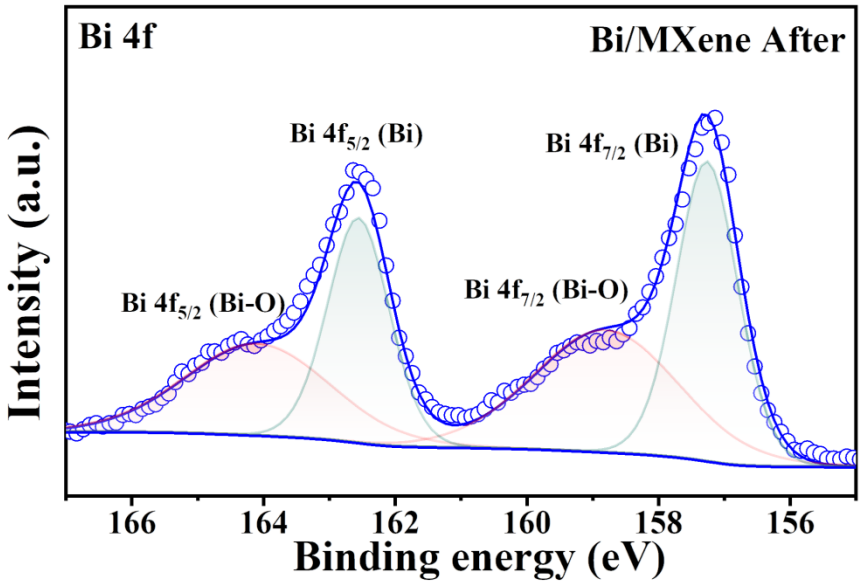

Fig. S15 XPS spectrum of the Bi 4f region for Bi/MXene after 1000 charge–discharge cycles.

4. References.

S1. X. Hui, R. Zhao, P. Zhang, C. Li, C. Wang and L. Yin, A*dv. Energy Mater.*, 2019, **9**, 1901065.

S2. H. Liang, C. Zhu, W. Tian, C. Zhu, Y. Ma, W. Hu, J. Wu, J. Chen, R. Wang and M. Huang, *Small*, 2024, **20**, 2400767.

S3 Y. Wang, T. Wu, Y. Lu, W. Zhang and Z. Li, *Angew. Chem.*, 2025, **137**, e202416032.